

USING EFFICIENT MODEL-BASED PARAMETER ESTIMATION FOR POLE-FREE SOLUTIONS OF MODAL PROPAGATION CONSTANTS, AS APPLIED TO SHIELDED PLANAR STRUCTURES

Robert Lehmensiek and Petrie Meyer

Department of Electronic Engineering, University of Stellenbosch, Stellenbosch, 7600, South Africa.

e-mail: lehmensk@ieee.org.

ABSTRACT: A fast and efficient adaptive sampling algorithm is applied to model-based parameter estimation of a Method-of-Lines implementation of two- and three-layer shielded planar structures, creating a pole-free function for the calculation of the propagation constants. The technique minimizes the number of characteristic equation evaluations, and hence reduces the computation time by orders of magnitude when compared to methods using the characteristic equation directly. Examples of a shielded microstrip line and a finline structure are shown. Between 3 and 15 evaluations of the characteristic function are typically required per determination of an imaginary or a real zero.

1. INTRODUCTION

The calculation of the propagation constants of modes in quasi-TEM microwave structures is a well-known problem in literature [1-5], and increasingly of interest in hybrid numerical analysis techniques incorporating Mode-Matching [6-8]. In the case of shielded planar structures, the two-dimensional Method-of-Lines (MoL) offers a very efficient analysis option, as it involves discretization in one direction only [9, 10]. However, in this method, as in many other formulations, the propagation constants of the modes are calculated by solving the function in equation (1), a severely non-linear function with an infinite number of solutions, normally interspersed with an infinite number of poles, together with very sharp non-zero local minima. For loss-less problems, the zeros can be purely real, purely imaginary or complex.

$$f(\gamma) = \det[Y(\gamma)] = 0. \quad (1)$$

As the existence of poles in the equation to be solved creates significant problems for most root-finding algorithms, a number of attempts to find pole-free solutions have been published. These include pole-free formulations [11], the use of a singular-value decomposition method (SVD) [12], and finding the pole-positions analytically and either removing them, as reported in [9], or searching between them [8]. Of these, the SVD method seems to produce the best results, at the cost of creating a function with a discontinuous first

derivative, making the use of fast gradient root-finding algorithms difficult.

Rational interpolation, specifically approaches using adaptive sampling algorithms, have been used by various authors to good effect in reducing the number of EM-evaluations for the determination of responses of microwave systems [13-19].

In this paper, an efficient model-based parameter estimation technique, based on a rational interpolation formulation, is used to provide an accurate, pole-free approximation to the roots of $f(\gamma)$. The technique uses a novel adaptive sampling algorithm to minimize the number of required EM-analysis points, and the resulting approximation can be written as the ratio of two polynomials, of which only the numerator needs to be solved for the zeros of the function. An added advantage of the polynomial representation is that the derivatives of the function can easily be calculated, enabling the use of gradient root-finding algorithms.

For the purposes of this paper, the technique is applied to the analysis of covered two- and three-layer planar structures, with the EM analysis performed by the two-dimensional MoL. The method is, however, not restricted to this specific formulation, but can be used for any analysis technique, which requires the solution of equation (1). It is shown that dramatic reductions in the number of evaluations of the characteristic function are achieved without loss of accuracy.

2. RATIONAL INTERPOLATION

Rational interpolation defines a function \mathfrak{R} of variable γ as a ratio of polynomials,

$$\mathfrak{R}(\gamma) = \frac{\sum_{k=0}^{\zeta} p_k \gamma^k}{\sum_{k=0}^{\nu} q_k \gamma^k} = \frac{N_{\zeta}(\gamma)}{D_{\nu}(\gamma)}, \quad (2)$$

with ζ the order of the numerator, ν the order of the denominator, and p_k and q_k the polynomial coefficients. We

assume $\mathfrak{R}(\gamma)$ exists for the function that we are trying to model. Since there are $\zeta+\nu+1$ unknown coefficients (q_0 is chosen arbitrarily), a set of $N+1=\zeta+\nu+1$ support points (γ_i, S_i) are required to completely determine $\mathfrak{R}(\gamma)$. $\mathfrak{R}(\gamma)$ is then a curve passing through the ordinates S_i at the abscissas γ_i for $i = 0, 1, \dots, N$.

The interpolation function $\mathfrak{R}(\gamma)$ can be calculated with the three-term recurrence relations given in equation (3) initialized with $N_0(\gamma) = S_0$, $D_0(\gamma) = 1$, $N_1(\gamma) = \varphi_1(\gamma_1, \gamma_0)N_0(\gamma) + (\gamma - \gamma_0)$ and $D_1(\gamma) = \varphi_1(\gamma_1, \gamma_0)$, and using the inverse differences defined in equation (4) [20].

The inverse differences, determined recursively from the support points, are the partial denominators of a continued fraction that represents $\mathfrak{R}_k(\gamma)$, and are essentially the polynomial coefficients defining $\mathfrak{R}_k(\gamma)$. The rational expressions $\mathfrak{R}_k(\gamma)$ are partial fractions of equation (2). As a consequence of the recursive equations used for k even $\zeta = \nu = \frac{k}{2}$ and for k odd $\zeta = \frac{k+1}{2}$ and $\nu = \frac{k-1}{2}$. Every new support point increases the order of the rational function by one, until $\mathfrak{R}(\gamma) = \mathfrak{R}_N(\gamma)$.

The derivative of $\mathfrak{R}_k(\gamma)$ with respect to γ can be calculated recursively by taking the derivatives of equation (3),

$$\begin{aligned} N_k(\gamma) &= \varphi_k(\gamma_k, \gamma_{k-1}, \dots, \gamma_0)N_{k-1}(\gamma) + (\gamma - \gamma_{k-1})N_{k-2}(\gamma) \\ D_k(\gamma) &= \varphi_k(\gamma_k, \gamma_{k-1}, \dots, \gamma_0)D_{k-1}(\gamma) + (\gamma - \gamma_{k-1})D_{k-2}(\gamma) \end{aligned} \quad \left. \begin{array}{l} \\ \\ \end{array} \right\} \quad k = 2, 3, \dots, N \quad (3)$$

$$\mathfrak{R}_k(\gamma) = \frac{N_k(\gamma)}{D_k(\gamma)} \quad k = 0, 1, \dots, N$$

$$\varphi_1(\gamma_i, \gamma_0) \equiv \frac{\gamma_i - \gamma_0}{S_i - S_0}, \quad i = 1, 2, \dots, N \quad (4)$$

$$\varphi_k(\gamma_i, \gamma_{k-1}, \dots, \gamma_0) \equiv \frac{\gamma_i - \gamma_{k-1}}{\varphi_{k-1}(\gamma_i, \gamma_{k-2}, \dots, \gamma_0) - \varphi_{k-1}(\gamma_{k-1}, \gamma_{k-2}, \dots, \gamma_0)}, \quad i = k, k+1, \dots, N; k = 2, 3, \dots, N$$

$$\begin{aligned} \frac{\partial N_k(\gamma)}{\partial \gamma} &= \varphi_k(\gamma_k, \gamma_{k-1}, \dots, \gamma_0) \frac{\partial N_{k-1}(\gamma)}{\partial \gamma} + (\gamma - \gamma_{k-1}) \frac{\partial N_{k-2}(\gamma)}{\partial \gamma} + N_{k-2}(\gamma) \\ \frac{\partial D_k(\gamma)}{\partial \gamma} &= \varphi_k(\gamma_k, \gamma_{k-1}, \dots, \gamma_0) \frac{\partial D_{k-1}(\gamma)}{\partial \gamma} + (\gamma - \gamma_{k-1}) \frac{\partial D_{k-2}(\gamma)}{\partial \gamma} + D_{k-2}(\gamma) \end{aligned} \quad \left. \begin{array}{l} \\ \\ \end{array} \right\} \quad k = 2, 3, \dots, N \quad (5)$$

$$\frac{\partial \mathfrak{R}_k(\gamma)}{\partial \gamma} = \frac{D_k(\gamma) \frac{\partial N_k(\gamma)}{\partial \gamma} - N_k(\gamma) \frac{\partial D_k(\gamma)}{\partial \gamma}}{D_k^2(\gamma)} \quad k = 1, 2, \dots, N.$$

initialized with $\frac{\partial N_0(\gamma)}{\partial \gamma} = 0$, $\frac{\partial D_0(\gamma)}{\partial \gamma} = 0$, $\frac{\partial N_1(\gamma)}{\partial \gamma} = 1$ and

$$\frac{\partial D_1(\gamma)}{\partial \gamma} = 0.$$

Similarly, all higher order derivatives of $\mathfrak{R}_k(\gamma)$ can be calculated.

As the accuracy of $\mathfrak{R}(\gamma)$ over a certain γ range is required to increase, the order of the interpolating rational polynomial increases. This increase in the degree of freedom of $\mathfrak{R}(\gamma)$ can cause a zero in the numerator and a zero in the denominator polynomials to occur at almost precisely the same position. At these pole/zero combinations L'Hospital's rule is applied for the evaluation of the interpolation function, i.e.

$$\mathfrak{R}_k(\gamma) \rightarrow \frac{\partial N_k(\gamma)}{\partial \gamma} / \frac{\partial D_k(\gamma)}{\partial \gamma}.$$

3. ERROR ESTIMATION AND ADAPTIVE SAMPLING ALGORITHM

Accurate rational interpolation of equation (1) requires that enough support points are used. In order to calculate the minimum number and the optimal position of these support points, a new adaptive sampling algorithm for application to the rational function approximation, as proposed by Lehmsiek and Meyer, is used [13]. A short exposition is repeated here for ease of understanding.

A natural residual term emerges from the rational interpolation formulation as $E_k(\gamma) = \frac{|\mathfrak{R}_k(\gamma) - \mathfrak{R}_{k-1}(\gamma)|}{1 + |\mathfrak{R}_k(\gamma)|}$,

which provides an estimate of the interpolation error. The residual decreases as k (or the degree of freedom of the function) increases and is zero at $k-1$ support points. The above-mentioned interpolation method is suitable as an adaptive sampling algorithm, since it produces an error estimate in a very natural way, and it works for unequally spaced support points.

The adaptive algorithm is defined to work in the interval $[\gamma_0, \gamma_1]$. As a first step, an arbitrary third support point γ_2 is selected which lies in the interval $[\gamma_0, \gamma_1]$. This point is required since the residual $E_1(\gamma)$ cannot produce an appropriate error estimate. The coefficient φ_1 for $\mathfrak{R}_1(\gamma)$ is determined from the support points (γ_0, S_0) and (γ_2, S_2) , while φ_2 for $\mathfrak{R}_2(\gamma)$ is recursively updated using equation (4) and the support point (γ_1, S_1) . The S_k 's are determined from the characteristic equation (1) at the γ_k 's. Define I_2 as the interval $[\gamma_0, \gamma_2]$. The residual $E_2(\gamma)$ is evaluated at a large number of equi-spaced sample points in the interval I_2 using equation (3). At the maximum of the evaluated sample points a new support point γ_3 is selected.

For iteration k the characteristic equation is evaluated at γ_k to determine S_k . Equation (4) calculates φ_k recursively. The residual $E_k(\gamma)$ is determined recursively at a large number of equi-spaced sample points on the interval I_k by using equation (3). Assuming the last support point (γ_k, S_k) was selected in the interval $[\gamma_b, \gamma_j]$, I_k is defined as both the intervals $[\gamma_0, \gamma_d]$ and $[\gamma_j, \gamma_1]$. The interval $[\gamma_b, \gamma_j]$ is excluded since it does not provide a suitable error estimate. This interval will decrease as the number of support points increase and it varies on alternate iterations. At the maximum of the evaluated residual a new support point (γ_{k+1}, S_{k+1}) is chosen. The process is repeated until the residual becomes arbitrarily small. By placing new support points at the approximate maximum of the residual $E_k(\gamma)$, this residual is minimized with respect to γ . The adaptive sampling algorithm automatically selects and minimizes the number of support points, and it does not require any *a priori* knowledge of the dynamics of the function in order to define an interpolation model $\mathfrak{R}(\gamma)$.

The number of equi-spaced evaluations of the residual is not crucial, as long as it is of an order larger than the number of support points. Placing the support points precisely at the maximum of the residual may sometimes slightly decrease the number of support points of the final model. However, the determination of such points through an iterative search algorithm is computationally expensive. It is important to note that for a full iteration, only one point is determined via the evaluation of equation (1). As all the other computation steps only require the evaluation of the interpolation function, the computational effort is decreased substantially.

The algorithm in [13] was developed for smoothly varying functions. When a very accurate interpolation model is required for an irregular function, such as in the case of equation (1), the number of support points can become large, causing the order of the rational polynomial to become large. This may cause the algorithm to become numerically unstable, especially with large function values. Therefore, the number of support points automatically selected by the adaptive sampling algorithm is limited to N_{bd} . If the sampling algorithm has not converged when this limit is reached, the support points in that interval are sorted in ascending order and subdivided into two new intervals. Each interval is initialized with $\frac{1}{2}(N_{bd}+1)$ support points if N_{bd} is odd, or $\frac{1}{2}N_{bd}+1$ and $\frac{1}{2}N_{bd}$ support points if N_{bd} is even. The support point at the cut is used as the last support point in the first interval and also as the first support point in the second interval. Hence all previously determined support points are reused, and more support points will be placed where needed. The intervals become smaller where the errors are larger. The adaptive sampling algorithm is repeatedly applied to each subdivided interval until every interval has attained convergence. The result is a set of interpolation models $\mathfrak{R}(\gamma)$ each defined on a specific interval of the complete band that is being modeled. Decreasing N_{bd} produces more accurate models at the expense of an increased number of $\mathfrak{R}(\gamma)$'s, an increased number of support points and increased computation time.

4. TWO-DIMENSIONAL METHOD-OF-LINES

The Method-of-Lines (MoL) was introduced to the field of numerical electromagnetic analysis in the early eighties and has since been established as a powerful method, especially for the analysis of planar structures. In essence, the two-dimensional MoL involves the discretization of the two-dimensional Helmholtz equation in only one direction. This results in a number of coupled differential equations, which are de-coupled using matrix techniques. The result is a number of uncoupled differential equations, each describing a transformed field or potential along a *line* instead of at a single point, hence the name Method-of-Lines. The elimination of discretization in one dimension is the key feature of the MoL and results in reduced computer storage requirements and reduced run-times. The two-dimensional MoL has been shown by numerous authors to be fast, accurate and effective.

For the determination of higher order modes on planar structures, the MoL offers a number of particular advantages:

- multi-layer structures are incorporated very naturally in the formulation,
- multiple conducting strips at various interfaces are incorporated with virtually no extra effort,
- shielded structures are handled with ease, and

- the final matrix to be solved contains only lines ending on or passing through conducting strips, and can be as small as 6x6 complex elements for a single microstrip line. It stands to reason, however, that the higher the number of modes required, the smaller the discretization distances should be.

The mathematical derivations of the MoL formulation are beyond the scope of this paper. The interested reader is referred to [10], and for explicit closed-form formulations for two- and three-layer structures, to [21, 22].

5. ROOT FINDING ALGORITHMS

The adaptive sampling algorithm determines, with the minimum number of evaluations of the characteristic equation (1), two sets of models, one for the real axis $\Re(\gamma = \alpha)$ and one for the imaginary axis $\Re(\gamma = j\beta)$. Although it is possible to determine a model $\Re(\gamma)$ in the complex γ -plane using the theory of section 3, such a model requires a large number of support points in order to achieve the required accuracy. As typical problems exhibit small numbers of zeros in the complex γ -plane, a constrained root finding algorithm is applied directly to the characteristic equation.

5.1 Real and imaginary axis

The root finding algorithm is repeatedly applied to each model (an analytic equation) on the real and the imaginary axes to determine all the propagation constants for both the propagating and evanescent modes respectively. Finding the roots is made exceptionally simple and efficient because:

1. The numerator of the rational polynomial can easily be calculated from equation (3), and is pole-free by nature.
2. The derivative of the numerator can easily be calculated from equation (5).
3. The evaluation of the numerator and its derivative are not computationally expensive.

Therefore, an iterative root finding algorithm can be applied to the models $\Re(\gamma)$. We used the first order Newton-Raphson method with a bisection search when the former failed [23], and the zero suppression technique [24] to prevent the root finding algorithm to converge to the same root twice. The maximum Newton-Raphson step size was limited to 10% of the search interval. The zero suppression technique implies that the derivative used in the Newton-Raphson method is changed to:

$$\frac{\partial N(\gamma)}{\partial \gamma} - \sum_{i=1}^{N_r} \frac{N(\gamma)}{\gamma - \xi_i}, \quad (6)$$

where ξ_i are the N_r previously found roots. The advantage of this technique, as opposed to deflation where the polynomial $N(\gamma)$ is divided by $\gamma - \xi_i$ explicitly so as to give a lower order

polynomial, is that the accuracy of a new root is not sensitive to the errors incurred in calculating the previous roots.

The root finding algorithm is initialized at the lowest γ value in the interval and forced to search in the positive γ direction until it reaches the highest γ value in the search interval. To ensure that roots on the border of the interval are found, the root finding algorithm is allowed to search past the highest γ value by 1% of the band.

The accuracy of the models $\Re(\gamma)$ is required to be high to ensure that the root positions of $\Re(\gamma)$ are accurate and that $\Re(\gamma)$ does not miss any roots, which are found in the characteristic equation (1). As was mentioned in section 3, this demand on accuracy can cause the adaptive sampling algorithm to produce pole/zero combinations, with the result that more zeros are determined than are present in the characteristic equation. We therefore test for the validity of all zeros found by the root finding algorithm. If the roots are closer than 10^{-3} to a pole, they are eliminated. The poles are found by doing a first order Newton-Raphson search of $D(\gamma)$ in the vicinity of the roots.

5.2 Complex plane

The complex conjugate roots, i.e. the complex propagation constants, in the complex γ -plane are found directly from the characteristic equation (1) by using a secant search method, which requires two characteristic equation evaluations per iteration. The search space is divided into a number of areas in the β direction. In each area the search is constrained within that area by dividing the characteristic equation by the following equation

$$(\alpha)(\alpha - \alpha_u)(\beta - \beta_l)(\beta - \beta_u), \quad (7)$$

and limiting the Newton-Raphson step size to fall within this area. α_u is the upper limit on the real axis, and β_l and β_u are respectively the lower and upper limits on the imaginary axis. Since the imaginary part of the complex roots is generally small, the size of the areas is progressively increased further away from the α -axis. The areas were allowed to slightly overlap to ensure that roots on the border are found.

The maximum step size was limited to 20% of the diagonal of the search area. Zero suppression is used as in section 5.1. In the α direction the algorithm was started at N_{st} different positions to prevent it from getting stuck in local minima and to allow it to search the whole area. The following starting positions were used:

$$\frac{2i+1}{2N_{st}} \alpha_u + j0.05(\beta_u - \beta_l) + \beta_u, \quad i = 0, 1, \dots, N_{st}-1 \quad (8)$$

6. EXAMPLES

The technique was tested on two examples: a shielded microstrip line structure and a centered slot unilateral fin line structure. For the adaptive sampling algorithm we chose the maximum order of the rational polynomial in an interval (N_{bd}) equal to 29. The residual $E_k(\gamma)$ in an interval was evaluated at 500 points and convergence was assumed when the maximum value of this residual was smaller than -80 dB. For the root finding algorithms the maximum number of iterations allowed until convergence was 30 and convergence was assumed when the step size was smaller than 10^{-5} . For the complex root finding algorithm the number of divisions in the β direction was chosen as three and N_{st} was chosen as 15 (closest to α -axis), 10 and 5 (furthest from α -axis) for the three areas.

6.1 Shielded microstrip line

The loss-less shielded microstrip line structure is shown in Fig. 1. The area in which to find the roots was chosen as $[0; j2.979]$ on the imaginary axis and $[0; 2]$ on the real axis. Only the even order modes are calculated and uniform discretization is used. Table 1 shows the support points selected by the adaptive sampling algorithm after every iteration for the microstrip line at 20 GHz. The propagation constants are normalized with respect to the free space wave number k_0 , i.e. $\gamma/k_0 = \alpha/k_0 + j\beta/k_0$. On the real axis the interval was divided into two intervals, α_1 and α_2 , when the number of support points reached 29. The shaded areas show the 29 support points before interval division. Both the maximum and the average relative errors after every iteration, and the roots found in each interval are shown.

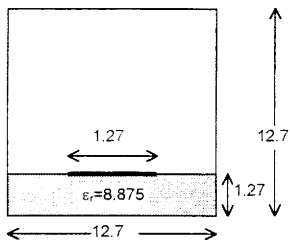


Fig. 1. Cross-section of the shielded microstrip line. All dimensions are given in millimeters.

Fig. 2 shows the interpolation model response and the support points for the model determined over interval α_2 . Fig. 3 shows the residual $E_k(\gamma)$ at convergence of the adaptive sampling algorithm and the relative error between the characteristic equation response and the interpolation model response, i.e. $\frac{|\det[Y(\gamma)] - \mathfrak{R}_k(\gamma)|}{1 + \det[Y(\gamma)]}$. Fig. 4 shows the

calculated numerator and denominator of the function of Fig. 2.

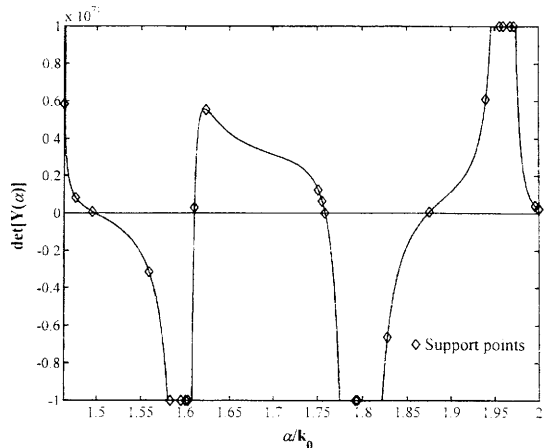


Fig. 2. The interpolation model response using the support points (diamonds) established by the adaptive sampling algorithm for the structure of Fig. 1 at 20 GHz. This is the second interval, i.e. α_2 , on the α -axis as chosen by interval division. Support points larger than $\pm 10^{-71}$ are shown at $\pm 10^{-71}$ respectively.

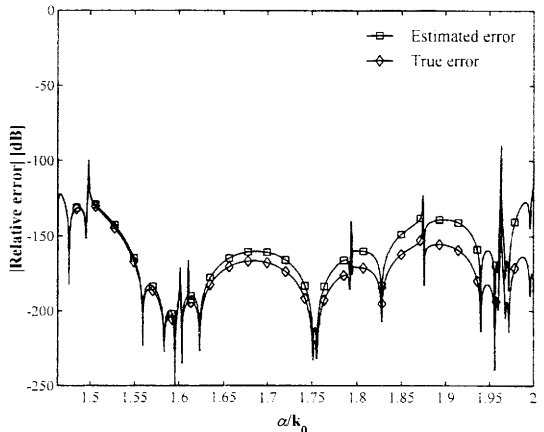


Fig. 3. The relative error estimated by the adaptive sampling algorithm at convergence and the relative error between the characteristic equation response and the interpolation model response (Fig. 2) at 20 GHz.

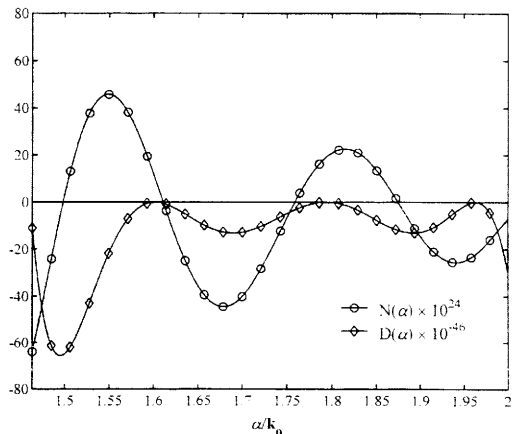


Fig. 4. The interpolation model response (Fig. 2) split into its numerator $N(\alpha)$ and the denominator $D(\alpha)$ components.

TABLE I Adaptive sampling algorithm iterations for shielded microstrip line (Fig. 1) at 20 GHz. The shaded areas show the support points used for initialization on the β -axis, and those determined before interval division on the α -axis. Propagation constants are normalized with respect to the free space wave number k_0 .

k	$j\beta \in [0; j2.979]$			$\alpha_1 \in [0; 1.463]$			$\alpha_2 \in [1.463; 2]$		
	Support points	$E_k(\gamma)$ [dB]		Support points	$E_k(\gamma)$ [dB]		Support points	$E_k(\gamma)$ [dB]	
		Max	Average		Max	Average		Max	Average
1	0			0			1.463		
2	j1.489			0.136			1.495		
3	j2.979	41.1	4.8	0.497			1.559		
4	j1.110	11.8	-22.6	0.589			1.583		
5	j2.877	-34.4	-47.9	0.625			1.595		
6	j1.098	4.5	-11.9	0.733			1.603		
7	j2.955	34.7	-5.0	1.000			1.623		
8	j2.782	75.7	27.2	1.034			1.876		
9	j1.260	30.1	6.3	1.066			1.940		
10	j2.633	39.2	3.0	1.106			1.956		
11	j0.680	-6.6	-38.6	1.194			1.960		
12	j2.394	37.7	-2.7	1.351			1.968		
13	j0.836	35.2	-4.2	1.367			1.972		
14	j0.573	20.5	-19.8	1.387			1.996		
15	j0.704	24.7	-13.4	1.463	-35.6	-50.2	2.000	32.5	-13.9
16	j0.495	68.2	16.7	0.551	25.0	-18.8	1.828	35.9	-1.3
17	j0.597	5.5	-18.9	0.243	-0.9	-48.4	1.476	43.2	3.2
18	j0.490	-0.8	-47.8	1.460	-48.7	-67.4	1.610	40.6	-2.9
19	j1.904	27.5	-6.9	0.067	-62.0	-81.9	1.756	-33.0	-64.8
20	j0.304	-47.0	-81.7	1.445	-65.7	-81.5	1.601	-14.3	-54.5
21	j0.806	-9.9	-55.5	0.023	-55.4	-72.4	1.792	-59.5	-84.8
22	j0.472	-40.3	-65.6	0.138	-70.5	-84.7	1.751	2.3	-40.1
23	j0.066	-53.4	-96.0	0.334	-83.0	-104.0	1.759	-58.6	-101.8
24	j0.424	-67.3	-105.0				1.794	-108.7	-139.2
25	j1.988	-95.9	-130.8						
<hr/>									
Roots found		j0.59457						1.4978	
		j0.72511						1.6102	
		j1.1027		0.55192				1.7589	
		j2.7106						1.8744	

TABLE II Propagation constant γ/k_0 of the first six even order modes for the microstrip line of Fig. 1 at 20 GHz.

	Mode 1	Mode 2	Mode 3	Mode 4	Mode 5	Mode 6
Huang [5]	j2.7086	j1.1031	j0.72499	j0.59418	0.55274	0.77162 ± j0.15345
This Method	j2.7106	j1.1027	j0.72511	j0.59457	0.55192	0.75304 ± j0.14338

The even order propagation constants γ/k_0 of the first six modes at 20 GHz are listed in Table II together with Huang's results [5]. Huang used the singular integral equation method to determine the propagation constants. Fig. 5 shows all the even order modes versus frequency. Evanescent modes $\gamma/k_0 = \alpha/k_0$ are plotted in the opposite direction.

The number of characteristic equation evaluations to determine all the propagation constants versus frequency is shown in Fig. 6 and Fig. 7 evaluated in increments of 0.1 GHz. The complexity of the function increases as frequency increases and so the number of characteristic equation

evaluations increase. From 16.4 GHz the number of divisions on the α -axis increases to two, and at 22.3 GHz and 23.0 GHz and from 23.2 GHz the number of divisions is three. Fig. 8 shows that between 3 and 15 evaluations are required per determination of an imaginary or a real root over the interval of interest. The calculation of roots via a previously published technique [8] required between 100 and 300 evaluations of the characteristic equation to determine the roots between adjacent poles. Note that the number of poles over the interval of interest is between 3 and 8, resulting in a typical reduction of a factor 100 in computational effort.

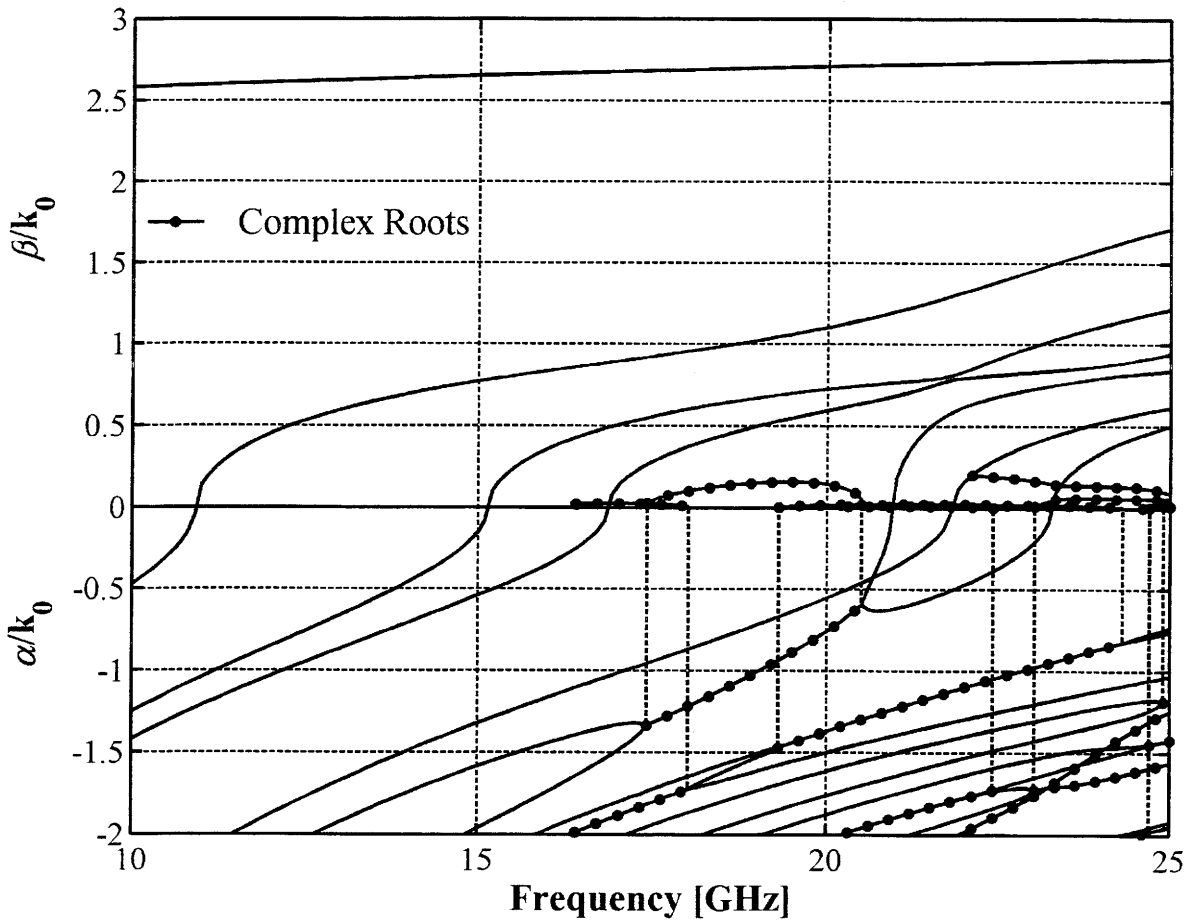


Fig. 5. Even order propagation constants $\gamma = \alpha + j\beta$ normalized with k_0 versus frequency for the structure shown in Fig. 1.

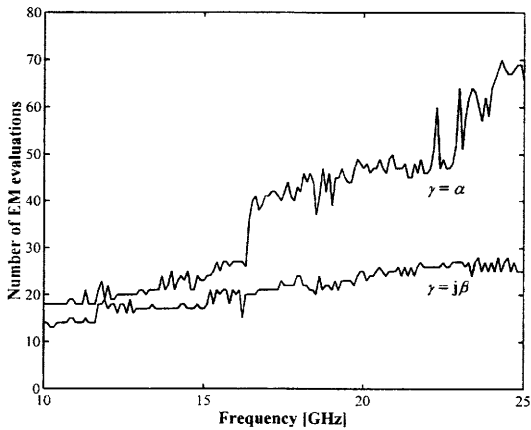


Fig. 6. The number of characteristic equation evaluations versus frequency required by the adaptive sampling algorithm to establish a model for both $\gamma = j\beta$ and $\gamma = \alpha$ for the structure shown in Fig. 1.

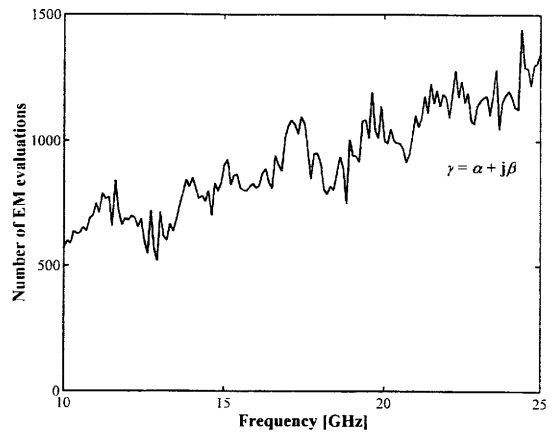


Fig. 7. The number of characteristic equation evaluations versus frequency required to determine the roots in the complex plane $\gamma = \alpha + j\beta$ for the structure shown in Fig. 1.

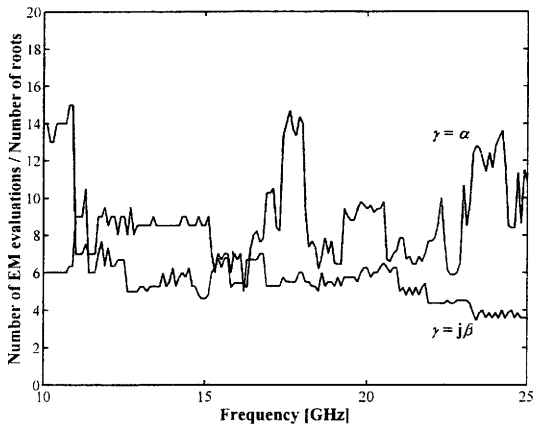


Fig. 8. The number of characteristic equation evaluations per number of roots found versus frequency for both $\gamma=j\beta$ and $\gamma=\alpha$ for the structure shown in Fig. 1.

6.2 Unilateral fin line

The guide wavelength λ is evaluated for the unilateral fin line with a centered slot as shown in Fig. 9. The wavelength inside the guide is $2\pi/\beta_0$, where β_0 is the dominant mode. The results are compared with those obtained in [25], where

spectral domain formulas and modal analysis were used. Fig. 10 shows the guide wavelength λ normalized with the free space wavelength λ_0 versus frequency for different values of the slot width, w . Table III compares the computed results with those given in [25, Table 4.4].

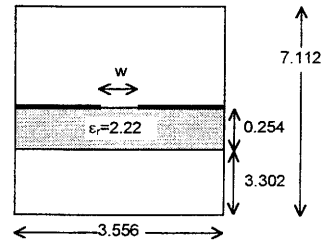


Fig. 9. Cross-section of the centered slot unilateral fin line. All dimensions are given in millimeters.

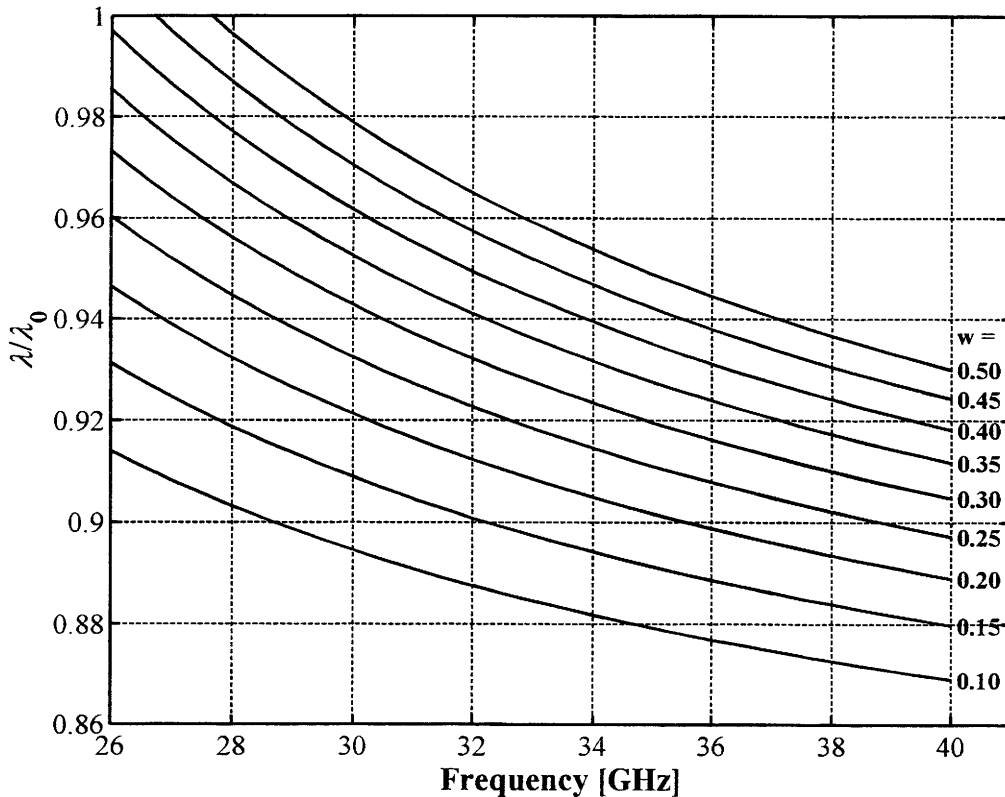


Fig. 10. Normalized guide wavelength λ/λ_0 versus frequency for the centered slot unilateral fin line shown in Fig. 9. w is given in millimeters.

TABLE III Comparison of the guide wavelength λ/λ_0 for the unilateral fin line of Fig. 9 with $w = 0.5$ mm.

Frequency [GHz]	λ/λ_0		
	Modal analysis [25]	Spectral domain [25]	This Method
26.0	1.1096	1.0200	1.0192
30.0	0.9791	0.9794	0.9789
35.0	0.9491	0.9494	0.9490
40.0	0.9302	0.9304	0.9301

7. CONCLUSION

The adaptive sampling algorithm efficiently determines the selection and the minimum number of propagation constant support points needed to accurately define a rational function model of the characteristic equation over the propagation constant range of interest. A root finding algorithm applied to the interpolation model is fast and efficient. The adaptive sampling algorithm added to the Method-of-Lines technique was applied to the analysis of a shielded microstrip line structure and a unilateral fin line structure, and required typically between 3 and 15 evaluations of the characteristic function to determine an imaginary or a real zero.

REFERENCES

- [1] D. G. Corr and J. B. Davies, "Computer analysis of the fundamental and higher order modes in single and coupled microstrip," *IEEE Trans. Microwave Theory Tech.*, vol. 20, pp. 669-678, Oct. 1972.
- [2] G. Essayag and B. Sauve, "Study of higher-order modes in a microstrip structure," *Electron. Lett.*, vol. 8, no. 23, pp. 564-566, Nov. 1972.
- [3] C. J. Railton and T. Rozzi, "Complex modes in boxed microstrip," *IEEE Trans. Microwave Theory Tech.*, vol. 36, pp. 865-874, May. 1988.
- [4] E. Anemogiannis, E. N. Glytsis and T. K. Gaylord, "Efficient solution of Eigenvalue equations of optical waveguiding structures," *J. Lightwave Technol.*, vol. 12, no. 12, pp. 2080-2084, Dec. 1994.
- [5] W-X. Huang and T. Itoh, "Complex modes in lossless shielded microstrip lines," *IEEE Trans. Microwave Theory Tech.*, vol. 36, no. 1, pp. 163-165, Jan. 1988.
- [6] R. Sorrentino and M. Mongiardo, "Efficient and versatile analysis of microwave structures by combined mode matching and finite difference methods," *IEEE Microwave and Guided Wave Lett.*, vol. 3, no. 8, pp. 241-243, Aug. 1993.
- [7] R. Beyer and F. Arndt, "The generalised scattering matrix separation technique combined with the MM/FE method for the efficient modal analysis of a comprehensive class of 3D passive waveguide circuits," *IEEE Int. Microwave Symp. Dig.*, Orlando, pp. 277-280, Jun. 1995.
- [8] P. Meyer, "Solving microstrip discontinuities with a combined mode-matching and Method-of-Lines procedure," *Microwave Opt. Technol. Lett.*, vol. 8, no. 1, pp. 4-8, Jan. 1995.
- [9] U. Rogge and R. Pregla, "Method of Lines for the analysis of dielectric waveguides," *J. Lightwave Technol.*, vol. 11, no. 12, pp. 2015-2020, Dec. 1993.
- [10] R. Pregla and W. Pascher, *Numerical techniques for microwave and millimetre-wave passive structures*, (editor T Itoh), New York: John Wiley and Sons, pp.380-446, 1989.
- [11] C. A. Olley and T. E. Rozzi, "Systematic characterisation of the spectrum of unilateral finline," *IEEE Trans. Microwave Theory Tech.*, vol. 34, pp. 1147-1156, Nov. 1986.
- [12] V. A. Labay and J. Bornemann, "Matrix singular value decomposition for pole-free solutions of homogenous matrix equations as applied to numerical modelling methods," *IEEE Microwave and Guided Wave Lett.*, vol. 2, no. 2, pp. 49-51, Feb. 1992.
- [13] R. Lehmensiek and P. Meyer, "An efficient adaptive frequency sampling algorithm for model-based parameter estimation as applied to aggressive space mapping," *Microwave Opt. Technol. Lett.*, vol. 24, no. 1, pp. 71-78, Jan. 2000.
- [14] E. K. Miller, "Model-based parameter estimation in electromagnetics: I—Background and theoretical development," *Applied Computational Electromagnetics Society Newsletter*, vol. 10, no. 3, pp. 40-63, Nov. 1995.
- [15] E. K. Miller, "Minimizing the number of frequency samples needed to represent a transfer function using adaptive sampling," *12th Annual Review of Progress in Applied Computational Electromagnetics*, Naval Postgraduate School, Monterey, CA, pp. 1132-1139, 1996.
- [16] T. Dhaene, J. Ureel, N. Faché, and D. de Zutter, Adaptive frequency sampling algorithm for fast and accurate S-parameter modeling of general planar structures, *IEEE Int Microwave Symp Digest*, Orlando, FL, May 1995, 1427-1430.
- [17] J. Ureel, N. Faché, D. de Zutter, and P. Lagasse, Adaptive frequency sampling of scattering parameters obtained by electromagnetic simulation, *IEEE AP Symp*, Vol. 2, (1994), 1162-1165.

- [18] R.S. Adve, T.K. Sarkar, S.M. Rao, E.K. Miller, and D.R. Pflug, Application of the Cauchy method for extrapolating/interpolating narrow-band system responses, *IEEE Trans Microwave Theory Tech*, Vol. 45, (1997), 837-845.
- [19] S.F. Peik, R.R. Mansour, and Y.L. Chow, Multidimensional Cauchy method and adaptive sampling for an accurate microwave circuit modeling, *IEEE Trans Microwave Theory Tech*, Vol. 46, (1998), 2364-2371.
- [20] J. Stoer and R. Bulirsch, *Introduction to numerical analysis*, Berlin: Springer-Verlag, 1980.
- [21] P. Meyer, "A combined mode-matching and Method-of-Lines procedure for the analysis of planar microwave circuits", Ph. D. Thesis, University of Stellenbosch, 1995.
- [22] W. J. A. van Brakel, "Solving three-layer planar microwave structures with the Method-of-Lines", Master Thesis, University of Stellenbosch, 1998.
- [23] R. Fletcher, *Practical methods of optimization*, Chichester: John Wiley & Sons, 1987.
- [24] G. Peters and J. H. Wilkinson, "Practical problems arising in the solution of polynomial equations," *J. Inst. Math. Appl.*, vol. 8, pp. 16-35, 1971.
- [25] B. Bhat and S. K. Koul, *Analysis, design, and applications of fin lines*, Norwood: Artech House Inc., 1987.